Extended release of dexamethasone from oleogel based rods

Russell Macoon[a], **Timothy Guerriero**[a], **Anuj Chauhan**[b,*]

[a]Department of Chemical Engineering; University of Florida; Gainesville, FL 32611

[b]Department of Chemical Engineering; Colorado School of Mines; Golden, CO 80401

Abstract

Hypothesis—Topical and systemic methods are not able to deliver ophthalmic drugs for treatment of retinal diseases. Consequently, invasive monthly intravitreal injections through the eyeball are required to deliver retinal drugs. A reduction in the frequency of the injection through extended release of the drugs could have significant clinical benefits.

Experiments—Oleogels containing ethyl cellulose as the gelator at 10% (wt%) in soybean oil were loaded with dexamethasone above the solubility limit and expunged from a syringe to create cylindrical rods for extended drug delivery. The devices were imaged to explore particle distribution and drug release was measured under sink conditions in buffer. A model was developed and fitted to data to determine effective drug diffusivity.

Findings—Dexamethasone is released slowly due to the presence of the drug particles that serve as drug depots. The release increases from 600 to 3000 hours as the drug loading is increased from 3% to 28%. The release profiles can be modeled by considering drug dissolution and diffusion, as well as the tortuosity of the matrix due to the presence of the voids formed after the drug particles have dissolved. The proposed approach is promising as the release profiles of the drug are comparable to commercial devices.
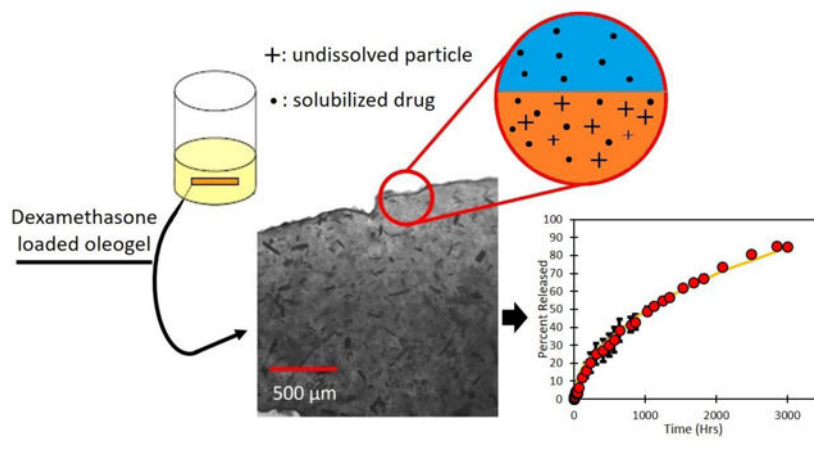
Graphical Abstract

*Corresponding author: Tel: +1 (303) 273-3539; chauhan@mines.edu, Address:1613 Illinois Street Alderson Hall Rm 251 Golden, CO 80401.
Address: 1006 Center Drive, PO Box 116005, Gainesville, FL 32611

II. Introduction

Ophthalmic drug delivery for treatment of retinal diseases represents a very large untapped market. According to a recent report from Allied Market Research, the global ocular drug technology market was worth $29.2 billion in 2016 and is predicted to increase to $42.7 billion by 2023. Retinal disorders including age-related macular degeneration (AMD) and diabetic macular edema (DME) are projected to be the major growth drivers in this segment [1]. A recent systematic review and meta-analysis predicts that approximately 196 million people worldwide will be afflicted by AMD by 2020 [2] and about 21 million people suffered from DME in 2014. The prevalence of DME is expected to increase to about 100 million by 2030 [3]. Furthermore, due to aging of the US population and in the majority of the world, posterior segment ophthalmic diseases will only become more prevalent. The prescribed drugs for these diseases include Kenalog; (Bristol Myers Squibb, New York, NY), pegaptanib (Macugen; OSI/Eyetech and Pfizer, New York, NY), bevacizumab (Avastin; Genentech, San Francisco); and ranibizumab (Lucentis; Genentech). Vascular endothelial growth factor (VEGF) trap (Regeneron; Tarrytown, NY) is currently under exploration for treatment of macular degeneration.

One of the major obstacles in treatment of posterior segment diseases is the barrier for delivery of drugs to the back of the eye. Systemic delivery is ineffective because of the large retina-blood barrier and topical delivery through eye drops is ineffective due to rapid clearance from tears and large barrier offered by the conjunctiva-sclera layers [4-7]. Currently most treatments for retinal diseases are based on intravitreal injections, which are invasive, and could lead to serious complications such as retinal detachment [8-11]. A number of approaches are under investigation for delivering drugs for retinal diseases including ocular inserts, sub-tenon injections, ionotophoresis, microneedles, sclera implants, etc. [12-14]. Eye drops are still considered a possibility even through the bioavailability is extremely low because of rapid clearance from the tears [15-17]. While each of these approaches is promising, there are problems associated with each including clinical complications, difficulty of device insertion, efficacy, costs, etc. [18-21].

Due to the bottlenecks of all these approaches, intravitreal injections are most commonly utilized for delivery drugs to retina [22]. The intravitreal injections are typically given once a month and usually require follow up visits a few weeks after the injection [23-25]. Such frequent injections increase patient discomfort, while also increasing cost and the possibility of infection or other more serious complications such as retinal detachment [26-29]. The monthly injections are necessary because the drugs delivered through the injection are cleared from the vitreous by multiple pathways including flow from the vitreous to the aqueous, and uptake by the cells lining the retina followed by degradation or clearance through the flow in the choroid [30]. The potential for side effects from injections has driven considerable research towards designing devices that can either be implanted in the eye or injected through an intravitreal injection. These devices are designed to release drugs for extended periods resulting in a significant decrease in the frequency of the injectio ns [31].

Current Drug Delivery Devices

RETISERT® is a commercially available implant loaded with 0.59 mg fluocinolone acetonide, and inert microcrystalline cellulose, polyvinyl alcohol (PVA), and magnesium stearate [32]. The device releases drug for about 30 months with an initial release of 0.6μg/day, which decreases to 0.3-0.4μg/day after the first month [33,34]. The device is 3 mm by 2 mm by 5 mm in size and structurally contains a fluocinolone acetonide tablet inside of a silicone elastomer cup [33,35]. The silicone cup contains a release orifice and also holds a polyvinyl alcohol membrane between the tablet and the orifice. When the device is surgically implanted into the vitreous, the high-water content of the vitreous hydrates the tablet, releasing some drug into the PVA solution, which then crosses the release orifice [36]. This device is non-biodegradable and therefore it must be either surgically removed, or left in the eye indefinitely. Patients who still require medication after all the drug is released from the device undergo a replacement procedure, in which the doctor can remove the old device, or simply implant a new device in another location in the eye. The doctor may choose to leave behind the used device to avoid trauma of surgery [37]. RETISERT® is priced at about 20,000 USD [38].

Iluvien® is another intravitreal device used to treat diabetic macular edema. Iluvien® is a 3.5mm length cylindrical tube with a 0.37mm diameter [32], containing 190μg of fluocinolone acetonide, which is released at a rate of about releases 0.23–0.45 μg/day 18 or 36 months [33]. Iluvien® is administered using an injection procedure with a 25-guage needle which can be done in an office-visit without stiches, similar to a regular intravitreal injection. The price for this device is about 8000 USD [38]. Iluvien® like RETISERT® is non-erodible and so must be removed via surgery or left in the vitreous indefinitely.

Ozurdex® is a cylindrical implant 6 mm in length and 0.46 mm in diameter [39] containing 0.7 mg of the active ingredient dexamethasone which is released over the course of 6 months [34,40] with maximum efficacy in the first three months [33]. The dexamethasone implant is preloaded into the applicator that has a 22 gauge needle tip for injection into the vitreous in an office visit using the shelved injection technique. The implant has been used in trials to treat central retinal vein occlusion (CRVO) macular edema, diabetic macular edema, and uveitis. The drug is contained in a NOVADUR® solid polymer drug delivery system

comprising of poly(lactic-coglycolic acid) (PLGA) polymer matrix [33], which renders it biodegradable [41, 42]. The price for this intravitreal implant is about 2000 USD [38].

Our proposed Drug Delivery Method

Gels are increasingly becoming the preferred formulation in many pharmaceutical, cosmetic, and food applications [43]. Gels are viscoelastic complex fluids [44] typically composed primarily of a liquid component and an added gelator that results in formation of a stabilized three-dimensional matrix [43, 45]. Gels are classified into hydrogels or organogels based on whether the liquid component is water or a non-polar liquid. Organogels can be further classified into amphiphilogels and oleogels. Amphiphilogels are created using surfactants, such as span 40 and tween 80, as both the solid and liquid components, and oleogels are formed using vegetable oils as the liquid phase [44,45].

Organogels are increasingly being used in the pharmaceutical industry as a vehicle for drug delivery [45]. Organogels have several key advantages over conventional delivery methods. They are relatively inexpensive and easy to prepare, can offer stability to emulsions and other liquid-based drug systems, are often thermoreversible, and are resistant to microbial contaminates [43,44]. Oleogel devices can also accommodate both hydrophilic or hydrophobic drugs. The shear-thinning properties allow the quasisolid oleogels to be easily applied topically, or by medical syringes [44]. Currently, use of gels commercially is limited to oral, nasal, dermal, and transdermal delivery, or parenteral injection [44]. We propose that these formulations are very promising for controlled release of ophthalmic formulations, both for the front and the back of the eye. Here we specifically focus on designing oleogel based formulations for delivery of drugs to the back of the eye by injecting the drug loaded oleogel into the vitreous. The high viscosity of the gel will help in retaining the shape, while also releasing the drug slowly. The slow dissolution of the oil itself will eventually lead to degradation of the injected oleogel-device. The designed oleogel is expected to be biocompatible because all components including oil and gelator have been previously used for biomedical applications.

In addition to using these formulations for intravitreal injections, it is also possible to use these for delivering medications to eyes through other routes including subconjunctiva injections, sub retinal injections, sub-tenon injections, retrobulbar injection, and suprachoroidal injection. It is also possible to use this approach for creating a device as a fornix implant that resides in the tears near the lower fornix continuously delivering drugs to the tears. Another possible use of this formulation is to create a punctum plug by injecting the formulation into the canaliculi through the puncta. Furthermore, oleogel formulations are not limited to use in the eye [46]. It is possible to use these formulations to give subcutaneous injections for delivering drugs to other parts of the body.

Design constraints for the oleogel based device

The design of the devices will eventually be dictated by a balance between safety and efficacy, which in turn will depend on the specific indications. As a starting point, we set the design targets based on currently commercialized devices Ozurdex® and Iluvien®. These devices are administered from 22 or 25 gauge needles and can create implants of different

masses. The oleogels themselves can be loaded with a variety of medication types, from hydrophobic to hydrophilic drugs, at a large range of desired concentrations. Here, we explore hydrophobic drug loading. The ease of changing the drug in the oleogel device promises for a myriad of uses commercially. In this study, the corticosteroid dexamethasone was used as a model hydrophobic drug.

There are many possibilities for the gelator molecule. Here we present results using ethyl cellulose as the gelator. Ethyl cellulose is biocompatible and suitable for use in pharmaceutics due to its inert character [47]. The vitreous humor lacks enzymes that can degrade ethyl cellulose, and so it may be cleared slowly via uptake into the retina cells or transport into the aqueous humor. There are other biocompatible gelators including proteins, phytosterols, waxes, sugar alcohols, and fatty acids that may be suitable alternatives [48-51].

There are many options for the liquid oily phase of the gel as well. Here, soybean oil was arbitrarily chosen amongst other edible oils for test formulations. The oils that are used have a very low solubility in vitreous humor. By adjusting the solubility, it is possible to obtain varying durations for which the devices remain in the vitreous. The duration can also be controlled by varying the concentration of gelator and/or drug concentration.

Based on the components used, the oleogel prepared here is expected to be biocompatible, though our specific formulation has not yet been approved for human use. Similar biocompatible drug loaded oleogels have been extensively researched [43.52,53] such as a canola oil/ ethyl cellulose oleogel explored for oral drug delivery applications [54].

III.   Materials and Methods

a.   Materials Used in Experiments

Soybean oil USP (Spectrum Chemical) was used as the oil phase for the oleogel formulations. Soybean oil used in experiments met United States Pharmacopeia standards for chemical purity. Ethyl cellulose used as the gelator was purchased from Sigma-Aldrich. Ethyl cellulose used was viscosity 90 cP in a 5% (w/w%) in an 80:20 solution of toluene/ ethanol, with 48.9% ethoxy content. Medical grade Gibco™ Phosphate Buffered Saline (PBS 1X) was obtained from Fisher Scientific. The drug dexamethasone (9α-fluoro- 16α-methyl- 11β, 17α, 21-trihydroxy-1,4-pregnadiene-3,20-dione), (purity: 99%) was obtained from Carbosynth Limited.

b.   Preparing Dexamethasone Loaded Oleogels

Oleogels were made by gelling soybean oil by addition of ethyl cellulose using methods that have been used previously for similar applications [55-57]. Ethyl cellulose powder was added to soybean oil at room temperature to a loading of 10% (w/w) which is within the range at which oleogels form. A minimum 5% loading of ethyl cellulose is required in order to form a semisolid formulation, and a greater than 33% ethyl cellulose loading will create a solid [55]. The mixture was stirred to disperse the powder. The vial was then heated to 160 °C, which is the melting point of ethyl cellulose for 10 minutes or until the oil became darker and ethyl cellulose particles were no longer visible. For control experiments with no drug, this mixture with oil and melted ethyl cellulose was set aside to gel at room

temperature. To achieve dexamethasone loaded gels, the vials were immediately placed on a hot plate set to 90 °C at which the mixture remains liquid. While continuing to stir the mixture, dexamethasone particles were slowly added to achieve the desired drug loadings of 30, 50, 100, 150, 280 or 400 mg/mL. After stirring, some of the dexamethasone has dissolved into the oil, while the excess drug remains in particle form dispersed throughout the ethyl cellulose/oil mixture. After sufficient stirring to ensure the drug was well-mixed, the formulation was poured into a syringe and cooled at room temperature to form an oleogel.

c. Drug Release Experiment

Oleogels with dexamethasone were loaded into 1 mL syringes fitted with 22 gauge needles (0.4 mm inner diameter). Drug devices of required mass were injected into a 20 mL vial filled with PBS 1X. Saline has been used by ophthalmologists as a biocompatible aqueous humor and vitreous substitute in vitreoretinal surgeries as well as by scientists in animal trials [58,59]. Samples were taken from vials periodically and analyzed using a ThermoSpectronic GENESYS ultraviolet–visible (UV-Vis) spectrometer to determine the drug concentration. Because standard solutions of dexamethasone in PBS 1X have a max absorbance peak at 241 nm [60,61], the spectra were obtained over the range of wavelengths 210 nm to 400 nm to ensure that the measured spectra reflected the spectra of the drug. Figure 1 shows the spectra of a 0.05 mg/mL standard dexamethasone in PBS 1X solution used for measurements. After measurement, the sample was returned to the vial. Each experiment was conducted in triplicates.

d. Imaging

The oleogel devices were imaged periodically at 2x magnification to visualize the overall appearance of the device and to visually observe whether the device degraded. To microscopically image a section of the formulation, a thin slice was cut perpendicular to the length of the expunged oleogel rod and placed on a microscope slide. The oleogel was also imaged in a light microscope to determine whether the drug added to the formulation dissolved completely or resulted in a dispersion of the drug particles. The solubility limit of the drug was determined as the concentration above which the added drug did not completely dissolve. The expunged oleogel devices were imaged periodically with a camera placed 10 cm above the vial to determine changes in the device over time.

e. Model

The drug concentration in the oleogels is chosen to be higher than the solubility limit and so it is expected that the cylindrical devices expunged from the syringe will contain undissolved drug particles. These systems can be modeled as cylinders containing undissolved drug particles which is the same configuration as explored previously for designing cylindrical conjunctival inserts of cyclosporin A [62]. Although the oil phase slowly dissolves into the fluid, this effect is neglected here for simplicity. Also, the external fluid is considered to be a sink due to the very large volume compared to the gel volume.

The dexamethasone dissolved in the inserts first diffuses out into the surrounding medium to lower the concentration of drug in the gel below the solubility limit. As oil phase drug

dissolves into the PBS 1X, large drug particles suspended in the gel begin to dissolve into the oil phase of the gel. These phenomena cause a depletion zone near the surface of the gel, which is an area within the device that is devoid of dexamethasone particles, as illustrated in Figure 2. We can assume that the concentration profile within the depletion zone follows the pseudo-steady state hypothesis because the high drug concertation results in slow dissolution compared to the time scale of diffusion in the shell.

The depletion zone, of thickness δ, is located at a distance $(R-\delta)$ from $r = 0$, where R is the total radius of the oleogel device. We hypothesize that the radial diffusive flux of dissolved drug causes the depletion zone thickness to increase by δ. If the time scale of dissolution is slower compared to the time scale for achieving steady state concentration profile in the annulus, the diffusion of drug in the shell can be modeled as steady state diffusion, i.e.,

$$\frac{d}{dr}\left(r\frac{dC}{dr}\right) = 0 \quad (1)$$

which has the general solution

$$C = A + B\ln r \quad (2)$$

where C is the concentration of drug in the shell of the device, and A and B are constants which can be determined using the boundary conditions

$$\text{at } r = (R - \delta), \quad C = C^* \quad (3)$$

$$\text{at } r = R, \quad C = 0 \quad (4)$$

where C^* is the solubility limit of drug in oil. Based on the data, the overall transport is limited by diffusion in the oleogel and so the boundary layer thickness in the PBS, δf, is assumed to be zero. Therefore, at the interface $r = R$, the concentration is equal to that in the bulk aqueous phase, which is zero in our experiments due to the sink conditions. Using these boundary conditions yields the following,

$$C = C^* \frac{\ln(\frac{r}{R})}{\ln(\frac{R-\delta}{R})} \quad (5)$$

and

$$\frac{dC}{dr} = \frac{C^*}{\ln(\frac{R-\delta}{R})}\frac{1}{r} \quad (6)$$

The mass balance at $r=R-\delta$ gives

$$C_p\frac{d\delta}{dt} = D\frac{dC}{dr} \quad (7)$$

which implies that the diffusive flux is generated by dissolution of the particles. Combining the mass balance from dissolution with equation (6), we get the following equation for determining the depletion zone thickness as a function of time

$$\frac{d\delta}{dt} = -D\left(\frac{C^*}{C_p}\right)\left(\frac{1}{\ln(\frac{R-\delta}{R})}\right)\frac{1}{(R-\delta)} \quad (8)$$

where C_p is the initial concentration of drug in the gel and D is the effective diffusivity of drug in the oleogel. Equation (8) is subject to the following initial condition

$$\delta(t=0) = 0 \quad (9)$$

The rate of drug transport from the oleogel to the fluid is given by

$$\frac{dM_f}{dt} = -D\frac{dC}{dr}2\pi RL \quad at\ r = R \quad (10)$$

where Mf is mass of drug and L is the length of the cylindrical device. The mass of drug in the fluid is the product of the fluid volume and the time dependent concentration C^b to yield the following,

$$\frac{dc_b}{dt} = \frac{-DC^*}{\ln(\frac{R-\delta}{R})}\frac{2\pi L}{V_b} \quad (11)$$

where V^b is the total volume of PBS, the release medium used in the experiment. The ordinary differential equations (8) and (11) are solved simultaneously using MatLab solver ODE45. The theoretical data modeled with these equations is fitted against experimental concentration versus time data to estimate effective diffusivity.

However, at short times, the depletion zone, δ, is significantly less than the radius R, so the Eq. (7) can be simplified to yield

$$\frac{d\delta}{dt} = D\frac{C^*}{C_p}\frac{1}{\delta} \quad (12)$$

which can be reduced to

$$\delta = \sqrt{2D\frac{C^*}{C_p}t} \quad (13)$$

This value for δ can be combined with equation (5) to model concentration of drug in the release medium at short time as

$$V_b\frac{dC_b}{dt} = \frac{DC^*}{\sqrt{2D\frac{C^*}{C_p}t}}2\pi RL \quad (14)$$

Dividing equation (14) by the initial mass of the drug in the gel

$$M_0 = \pi R^2 LC_0 \quad (15)$$

where M_o is the initial mass of drug in the gel, gives the fractional release of drug at any short time

$$f = 2\sqrt{\frac{2D\,C^*t}{R^2C_p}} \quad (16)$$

where f is the fractional release of drug. Equation (16) can be fitted against short time experimental data to estimate the effective diffusivity D.

In the gel formulations in which the loading was below the solubility limit, drug completely dissolved into the oil phase, and therefore no particles were present. For these formulations, drug release follows a simple cylindrical diffusion model. It can be assumed that the diffusion is one directional because the length of the device is much longer than the radius.

$$D\frac{\partial^2 C}{\partial r^2} + \frac{D}{r}\frac{\partial C}{\partial r} = \frac{\partial C}{\partial t} \quad (17)$$

where $C(r, t)$ is the total drug concentration in the oleogel at position r and time t. Using a separation of variables method, this equation reduces to

$$\frac{d^2u}{dr^2} + \frac{1}{r}\frac{du}{dr} + \alpha^2\, u = 0 \quad (18)$$

which is a Bessel's equation of order zero. Solutions for equation (18) can be obtained in terms of Bessel's equations which satisfy boundary conditions. Concentration profiles can be solved given the boundary conditions

$$C = 0 \quad at\, r = R\, and\, t \geq 0 \quad (19)$$

$$C = C_p \quad at\, 0 < r < R\, and\, t = 0 \quad (20)$$

where C_p is the initial loading concentration of drug in the gel. The boundary condition (19) is satisfied by

$$C = \sum_{n=1}^{\infty} A_n J_0(\alpha_n\, r)\exp(-D\,\alpha_n^2\, t) \quad (21)$$

where α_n are the roots to

$$J_0(R\,\alpha_n) = 0 \quad (22)$$

With an initial uniform concentration C_p, the solution to equation (17) is

$$\frac{C - C_p}{C_0 - C_p} = 1 - \frac{2}{R}\sum_{n=1}^{\infty}\frac{\exp(-D\,\alpha_n^2\, t)J_0(r\,\alpha_n)}{\alpha_n\, J_1(R\,\alpha_n)} \quad (23)$$

for all cases in which the drug loading is lower than solubility limit.

IV.   Results and Discussion

Gel Properties

The solubility of dexamethasone in the oil phase was determined by preparing oleogels with different concentrations of drug and observing the samples under a microscope to determine the concentration above which particles were observed. The solubility of dexamethasone in soybean oil was determined to be 30 mg/mL (Table 1). For comparison, solubility of dexamethasone in saline is also included in the table.

The density of the drug loaded oleogels is important because it will impact the settling of the device after injection into the vitreous. The density of the devices loaded with 3, 5, 10, 15, 28 and 40% (w/w) drug were 0.950, 0.957, 0.975, 0.993, 1.04, and 1.083 g/mL, respectively. Once expunged, the devices dissolve very slowly, limited by the minute solubility of oil in aqueous solution. The ethyl cellulose backbone of the oleogel does not degrade, and devices have been observed to remain stable in solution for 30 months. During the gelation process, the ethyl cellulose remains stable at the 160 °C temperature required to induce melting. Thermogravimetric profiles show that substantial mass loss and degradation does not occur until well above 300 °C for soybean oil [65] and 200 °C for ethyl cellulose [66].

Imaging

Figure 3A-C show snapshots of the drug-loaded oleogel device at various times after expunging into a fluid reservoir. The devices maintain the cylindrical shape for the entire duration due to the high viscosity. Figure 3D is the 2X magnified image of the formulation showing a high concentration of rod like particles in the gel. Arrows in Figure 3(A, B, C) point to the oleogel devices and that in 3D point to the particles.

To illustrate the size of our device in comparison with the existing devices, Figure 4 shows a dexamethasone oleogel which has been expunged on a human thumb. The oleogel device's size can change depending on needle gauge and total mass of the injected formulation. In our experiments, a 22 gauge needle (0.413 mm diameter) was chosen and the length of the rod was set by the total volume required (3 mm – 22 mm). The RETISERT® implant is rectangular in shape, and is 3 mm by 2 mm by 5 mm in size [35]. Iluvien® is a 3.5 mm length cylindrical tube with a 0.37mm diameter [32]. The cylindrical biodegradable implant Ozurdex® is 6 mm in length with a 0.46 mm diameter [39].

Drug release profiles

The rate of drug release from the oleogels expunged into the phosphate buffered saline (PBS) was measured by taking samples periodically and determining the drug concentration by UV-Vis spectroscopy. The volume of the fluid (3-15 mL) was significantly larger than the volume of the oleogel device (0.0009 - 0.0038 mL) so the release medium can be considered to be a sink even for the very hydrophobic drugs. The mass of drug in the devices varied with the loadings with 700 μg of drug loaded in the device with 28% loading. The dynamic concentrations were used to calculate the fraction of the drug that is released. To explore the effect of particle loading on release profiles of dexamethasone, multiple loading concentrations including at or near solubility limit (3% and 5% dexamethasone loading) and well above solubility limit (10%, 15%, and 28% dexamethasone loading) were examined. The release profiles and release rates per day are plotted in Figure 5. Figure 5A shows a profile of a loading below solubility limit and Figures 5 (B, C, D, E, F) show loadings above the solubility limit. The error bars in the data are standard deviation of three independent experiments.

The final measured concentration of drug in solution was 6.7 μg/mL for the 3% drug loading device, 14.6 μg/mL for the 5% drug loading device, 38 μg/mL for the 10% drug loading device, 38.4 μg/mL for 15% drug loading device, 58.5 μg/mL for the 28% drug loading

device, and 20 µg/mL for the 40% drug loading device. For all studies, the final measured concentration of dexamethasone in solution is much higher than the maximum 1.11 ± 0.294 µg/mL concentration in vitreous observed in Ozurdex® animal trials [67]. Although Ozurdex® has been accepted for patient use by the FDA [68], dexamethasone at these concentrations may cause some side effects, including ocular hypertension, cataract, vitreous hemorrhage, and exacerbation or reoccurrence of ocular infections [69]. The toxicity of the dexamethasone oleogel formulations *in vivo* must be studied to determine the therapeutic window of our devices. Further optimization of drug loading concentration as well as device size can ensure that we balance efficacy with safety.

The devices with drug loading of 3% and 5% release drug for about 600 and 1400 hours respectively, which is substantially less than the release durations from the devices with higher drug loadings. For example, the 28% dexamethasone device released 85% after about 3000 hours and 40% device released 47.6% after 2660 hours. The long release duration suggests a low solubility of dexamethasone in the oil phase, which is supported by the microscopic images showing a high fraction of particles. The drug particles act as depots that dissolve as the drug concentration decreases below the solubility limit due to diffusion into the surrounding medium. The release can thus be described by Higuchi model for drug particles dispersed in an ointment, which suggests that the release duration should depend on the ratio of the drug loading and the solubility limit. The figures also include theoretical fits based on the diffusion equation for the system in which the initial loading is below the solubility limit and the Higuchi model developed earlier for the cases in which the initial loading is above the solubility limit (Eq. 11). The values of diffusivities obtained for each case are included in the figures. The diffusivity obtained from the gels below the solubility limit are within the margins of experimental error. However, the diffusivities obtained from the gels with higher drug loadings are lower significantly by more than an order of magnitude, which suggests that the model does not accurately represent the system developed here. We hypothesize that voids which form in the gel as particles solubulize into the oil phase act as additional mass transport barriers. These voids are not considered in the modeling equations, but may have an integral role in governing release duration. This role may become increasingly apparent as the initial loading concentration of drugs is increased because the number of voids will also increase.

Void Formation

Deviation from a purely Higuchi modeled drug release may be due to the formation of voids within the oleogel device. As the drug solubilizes into the oil phase and releases from the device, cavities form in the spaces which were once occupied by particles. Because of the high viscosity of the formulation, the oil phase cannot conform to fill these voids. The voids are likely filled with air or water. Transport of water through the oleogel is very slow due to low solubility so the voids likely contain air. Figure 6 shows microscopic images of a dexamethasone drug loaded gel before (6A) and after (6B) void formation. As a simple means of establishing that the dark regions in Figure 6B are voids, we melted the gel in 6B and then allowed it to solidify to form the gel. It was hypothesized that as the gel melts, it becomes less viscous allowing air voids (bubbles) to aggregate and rise out of the formulation to yield a clear gel, which is consistent with the image in Figure 6C. It is noted

that we did not observe any water drops when the oleogel with voids was melted further suggesting that the voids contain air.

Voids in the gel act as an additional transport barrier for drug release reducing the total area available for transport and increasing the tortuosity. Transport barriers which increase tortuosity in drug release has been previously discussed [70]. Additionally, as voids form around imbedded particles, the surface contact area between the particles and the oil phase of the gel diminishes, which could lead to additional decrease in release rates, but only if the release rates are controlled by particle dissolution and not by diffusion through the gel. At very high drug loadings, these factors could potentially even lead to particles which remain trapped in the gel resulting is only a partial release of the drug. The effects of the voids could be incorporated into the model by defining an effective diffusivity,

$$D_{eff} = D\frac{\varepsilon}{\tau} = D\frac{1 - \varnothing - \varnothing_s}{\tau} \quad (24)$$

where D is the molecular diffusivity in the gel, φ is the particle loading, $\varnothing_S$ is the solubility limit, ε ($= 1 - \varphi - \varnothing$) is the porosity and τ is the tortuosity [71,72]. With increasing particle loading, the porosity decreases and the tortuosity increases, which leads to a significant decrease in the effective diffusivity [73,74]. The molecular diffusivity in the gel is the fitted value from the loading below the solubility limit, and D_{eff} is the fitted diffusivity from the gels loaded with drug above the solubility limit. The data for the D_{eff} can be utilized to calculate the tortuosity for each particle loading by using Eq. (24). The dependency of the tortuosity on the porosity is shown in Figure 7. The dependency of tortuosity on porosity have been extensively explored in the context of effective mass transfer in packed beds, It is expected that the tortuosity should approach as the particle fraction reaches zero, i.e., the porosity reaches one. The data in Figure 8 shows a decreasing trend in tortuosity as the particle fraction decreases but does not appear to reach a limit of zero as porosity approaches one. The most likely reason is potential underestimation of the diffusivity for the lower particle loadings as evident from the poorer fits of the data in Figure 5 B-C compared to D-F.

Comparison of dexamethasone release at different initial loading

We explored many different drug loadings of dexamethasone and their effect on release duration. In order to easily compare these releases, the data from various experiments are compared in Figure 8 for all formulations that contain dexamethasone. This is the same data as shown in the previous sections but it is plotted as fractional drug release as a function of time to clearly illustrate the dependency of the release duration on the drug loading. The data for 40% loading is shown for longer duration compared to that in Figure 5 to show that the release rates decrease considerably after about 1600 hrs. We hypothesize that the high particle loading creates close to a percolating network of voids that leads to significant slowdown in the drug release. Thus, a loading of 28% may be most appropriate for this system.

The results reported above are very encouraging particularly for high loadings of dexamethasone, exhibiting release durations of a few months. The drug loading for dexamethasone is comparable to that for currently commercialized devices. The release rate could possibly be slowed down more by identifying an oil into which the drug dissolves to a lesser extent such as medium-chain triglycerides. In fact, solubility limit of drugs in the oil is the most important parameter for the drug release, so choosing a suitable oil can lead to extended release for other drugs as well. If the oil with the low solubility is not a good choice for gelation, a mixture of oils can be used, with one oil chosen based on solubility criterion and the other chosen to achieve gelation. The choice of oil is critical also to achieve controlled dissolution of the device. Ultimately it is preferable if the device disintegrates through dissolution of the oil and clearance from the vitreous. It is preferable thus to choose oil with a low but finite solubility in vitreous such as ethyl butyrate. The choice and concentration of the gelator is important to ensure biocompatibility and also maintain the gel after injection into the eye.

V. Conclusion

The results show that oleogels are promising for delivering ophthalmic drugs particularly to the back of the eye. The oleogel based devices can achieve similar release performance as commercial devices such as Ozurdex® and Iluvien® [11, 33, 34, 38,40, 42]. Some of the oleogel devices examined provided extended drug release of several months. These formulations, when optimized for patient use, would significantly reduce the frequency of injections from monthly [75, 76] to quarterly, or even bi-annually, reducing the potential for retinal damage as well as costs. Using several different drug loadings, we have shown that the release profile of dexamethasone is largely dependent on initial drug loading. The release of drugs from the oleogel devices can be modeled accurately if the effect of the voids created by dissolution of the particles are accounted through a tortuosity factor. The tortuosity is useful in further increasing the release duration. Though the proposed oleogel devices achieve similar release durations to current sustained-release steroid implants, the proposed method is encouraging because of its flexibility to easily accommodate a host of different drug particles. Thus, this work is an exciting improvement on existing devices, which are often only manufactured for specific drugs [77]. Another advantage to this formulation is its ability to be administered as an intravitreal injection. The procedure could be performed by a retina specialist in a clinic setting using only topical anesthetics and a sterile technique [78,79]. In this work we used the biocompatible gelator ethyl cellulose. While it may be cleared slowly via uptake into retina cells or transport into the aqueous humor, future studies may explore other biocompatible oleogel gelators including proteins, phytosterols, waxes, sugar alcohols, and fatty acids [48-51] and their effect on dissolution. A controlled, complete dissolution of the oleogel formulation after injection may be preferable to commercially available RETISERT® and Iluvien®, which are non-biodegradable, and may remain in the eye indefinitely [80]. It is noted that the release profile from the device developed here is not linear. While zero order release is desirable, it is not a requirement as long as the concentration can be maintained within the therapeutic window. While these systems are promising, considerable future work is needed to optimize the oleogel formulations for specific indications, and testing safety and efficacy in animal models.

## Acknowledgements

VII. References

1. Sapatnekar T, Chandra G Ophthalmic Drugs Market by Indication, Type, Dosage Form, Technology, Distribution, and Therapeutic Class - Global Opportunity Analysis and Industry Forecast, 2017-2023. Allied Market Research. (2017). https://www.alliedmarketresearch.com/ophthalmic-drugs-market.

2. Wong WL, Xinyi Su, Xiang Li, Chui Ming G Cheung, Ronald Klein, Ching-Yu Cheng Tien Yin Wong. Global prevalence of age-related macular degeneration and disease burden projection for 2020 and 2040: a systematic review and meta-analysis. The Lancet Global Health. (2014)2, #2:el06–el16.

3. Wolf S Diabetic macular oedema and the importance of vascular endothelial growth factor therapies in its treatment. European Ophthalmic Review. (2014) 8,:53–60

4. Sekar P Chauhan A Effect of vitamin-E integration on delivery of prostaglandin analogs from therapeutic lenses. Journal of Colloid and Interface Science. (2019) 539,:457–467. [PubMed: 30611041]

5. Ciolino J, Hoare T, Iwata N, et al. A Drug-Eluting Contact Lens. Investigative. Ophthalmology and. Vision Science. (2009) 50,#7:3346–3352. doi: 10.1167/iovs.08-2826.

6. Peng CC., Chauhan A Extended cyclosporine delivery by silicone-hydrogel contact lenses. Journal of Controled Release. (2011) 154, #3:267–274.

7. Hosoya K, Tachikawa M Inner Blood-Retinal Barrier Transporters: Role of Retinal Drug Delivery. Pharmaceutical Research. (2009) 26, #9:2055–2065. [PubMed: 19568694]

8. Moshfeghi D, Kaiser P, et al. Acute endophthalmitis following intravitreal triamcinolone acetonide injection. American Journal of Opthalmology. (2003) 136, #5:791–796.

9. Gillies M, Simpson J, Billson F, et al. Safety of an Intravitreal Injection of Triamcinolone: Results from a Randomized Clinical Trial. Arch Ophthalmol. (2004) 122, #3:336–340. [PubMed: 15006845]

10. Karabag Revan Yildirim et al. "Retinal tears and rhegmatogenous retinal detachment after intravitreal injections: its prevalence and case reports. " Digital Journal of Ophthalmology : DJO (2015) vol. 21 #1:8–10. 23 3. 2015, doi:10.5693/djo.01.2014.07.001 [PubMed: 27330458]

11. Falavaijani K, Nguyen Q Adverse events and complications associated with intravitreal injection of anti-VEGF agents: a review of literature. Eye (Lond). (2013). 27, #7:787–794. doi:10.1038/eye. 2013.107 [PubMed: 23722722]

12. Loftsson T, Hreinsdóttir D, Stefánsson E Cyclodextrin microparticles for drug delivery to the posterior segment of the eye: aqueous dexamethasone eye drops. Journal of Pharmacy and Pharmacology. (2007) 59, #5:629–635. [PubMed: 17524227]

13. Eljarrat-Binstock E, Domb A Iontophoresis: A non-invasive ocular drug delivery. Journal of Controlled Release. (2006) 110, #3:479–489. [PubMed: 16343678]

14. Moffatt K, Wang Y, Singh T, Donnelly R Microneedles for enhanced transdermal and intraocular drug delivery. Current Opinion in Pharmacology. (2017) 36, 14–21. [PubMed: 28780407]

15. Tahara K, Karasawa K, Onodera R, Takeuchi H Feasibility of drug delivery to the eye's posterior segment by topical instillation of PLGA nanoparticles. Asian Journal of Pharmaceutical Sciences. (2017) 12, #4:394–399.

16. Gupta H Updates on drug bioavailability and delivery to posterior segment of eye. Journal of Pharmacy & Bioallied Sciences. (2013) 5,#3:173–174. [PubMed: 24082691]

17. Loftsson T, Stefanasson E Cyclodextrins and topical drug delivery to the anterior and posterior segments of the eye. International Journal of Pharmaceutics. (2017) 531, #2:412–423.

18. Shoeibi N, Mahdizadeh M, Shafiee M Iontophoresis in ophthalmology: A review of the literature. Reviews in Clinical Medicine. (2014) 1, #4:183–188.

19. Custer P, McCaffery S Complications of Sclera-Covered Enucleation Implants. Ophthalmic Plastic & Reconstructive Surgery. (2006) 22, #4:269–273. [PubMed: 16855498]

20. Astbury N, Nyamai LA. Detecting and managing complications in cataract patients. Community Eye Health. (2016) 29, #94:27–29. [PubMed: 27833260]

21. Thakur Singh R, Tekko I, McAvoy K, McMillan H, Jones D, Donnelly R Minimally invasive microneedles for ocular drug delivery, Expert Opinion on Drug Delivery. (2017) 14, #4:525–537. DOI: 10.1080/17425247.2016.1218460. [PubMed: 27485251]

22. Lau P, Jenkins K, Layton C, Current Evidence for the Prevention of Endophthalmitis in Anti-VEGF Intravitreal Injections. Journal of Ophthalmology. (2018) 18,:8567912. doi: 10.1155/2018/8567912

23. Ferreira A, Sagkriotis A, Olson M, Lu J, Makin C, Milnes F Treatment Frequency and Dosing Interval of Ranibizumab and Aflibercept for Neovascular Age-Related Macular Degeneration in Routine Clinical Practice in the USA [published correction appears in PLoS One. (2015) 10, #8:e0136515], PLoS One. (2015) 10, #7:e0133968. doi:10.1371/journal.pone.0133968 [PubMed: 26208030]

24. Frampton J Aflibercept for Intravitreal Injection In Neovascular Age-Related Macular Degeneration. Drugs and Aging. (2012) 29, #10:839–846. [PubMed: 23038609]

25. Siegel M, Hughes B, Juzych M, Alexander M, Goyal A, Wolfe S, Kim C Effect of Intravitreal Bevacizumab (Avastin) on Intraocular Pressure in Patients With and Without Glaucoma. Investigative Ophthalmology and Vision Science. (2009) 50, #13:2485.

26. Meyer C, Michels S, Rodrigues E, Hager A, Mennel S, Schmidt J, Helb H, Farah M Incidence of rhegmatogenous retinal detachments after intravitreal antivascular endothelial factor injections. Acta Ophthalmologica. (2011) 89,:70–75. doi:10.1111/j.1755-3768.2010.02064.x [PubMed: 21176118]

27. Moshfeghi A, Rosenfeld P, Flynn HW Jr., et al. Endophthalmitis after intravitreal antivascular endothelial growth factor antagonists: A six-year experience at a university referral center. Retina. (2011) 31, #4:662–668. [PubMed: 21836400]

28. Day S, Acquah K, Mruthyunjaya P, Grossman D, Lee P, Sloan F Ocular complications after anti-vascular endothelial growth factor therapy in Medicare patients with age-related macular degeneration. American Journal of Ophthalmology. (2011) 152, #2:266–272. [PubMed: 21664593]

29. Chong D, Anand R, Williams Patrick., Qureshi J, Callanan D Characterization of Sterlile Intraocular Inflammatory Responses After Intravitreal Bevacizumab Injection. Retina. (2010) 30,#9:1432–1440. [PubMed: 20559156]

30. del Amo Eva M., Rimpelä A, Heikkinen E Kari O, et al. Pharmacokinetic aspects of retinal drug delivery. Progress in Retinal and Eye Research. (2017) 57, :134–185. [PubMed: 28028001]

31. Tian J, Liu J, Liu X, Xiao Y, Tang L Intravitreal infusion: A novel approach for intraocular drug delivery. Scientific Reports. (2016) 6,:37676. doi:10.1038/srep37676. [PubMed: 27886224]

32. Falavaijani K Implantable Posterior Segment Drug Delivery Devices; Novel Alternatives to Currently Available Treatments. Journal of Ophthalmic & Vision Research. (2009) 4, #3: 191–193. [PubMed: 23198073]

33. Haghjou N, Soheilian M, Abdekhodaie M Sustained Release Intraocular Drug Delivery Devices for Treatment of Uveitis. J Ophthalmic Vis Res. (2011) 6:4, 317–329. [PubMed: 22454753]

34. Lopez A, Albini T Therapeutic Options for Uveitis. Retina Today. (10 2017)

35. Del Amo E, Urtti A Current and future ophthalmic drug delivery systems: A shift to the posterior segment. Drug Discovery Today. (2008) 13, #3,4:135–143. [PubMed: 18275911]

36. "Long Term Continuous Control." Treatment of Chronic Non-infectious Uveitis - RETISERT®, Bausch and Lomb. http://www.retisert.com/product-information

37. Issue: Care of Patients with Chronic Noninfectious Posterior Uveitis. Retinal Physician. (3 2011).

38. Cabera M, Yeh S, Albini T Sustained-Release Corticosteroid Options. Journal of Ophthalmology. (2014) 2014 Article ID 164692

39. Kumar A, Ambiya V, Kapoor G, Arora A Wandering Ozurdex in eyes with scleral fixated intraocular lens and its management: A report of two cases. Journal of Current Ophthalmology. (2018) ISSN 2452-2325.

40. Lowder C, Hollander D Review of the Drug-infused Eye Implant—Ozurdex®® (Dexamethasone Intravitreal Implant). US Ophthalmic Review. (2011) 4:2:107–12

41. Pacella F, Ferraresi AF, Turchetti P Intravitreal Injection of Ozurdex®® Implant in Patients with Persistent Diabetic Macular Edema, with Six-Month Follow-Up. Ophthalmol Eye Dis. (2016) 4 28:8:11–6. [PubMed: 27147895]

42. Kiss S Sustained-release Corticosteroid Delivery Systems. Retina Today. (2010) May-Jun 44–46.

43. O'Sullivan C, Barbut S, Marangoni A Edible oleogels for the oral delivery of lipid soluble molecules: Composition and structural design considerations. Trends in Food Science & Technology (2016) 57:59–73.

44. Mishra M Handbook of encapsulation and controlled release. Boca Raton: CRC Press/Taylor & Francis Group, 2016 1035–1060. Print.

45. Rehman K, Zulfakar M Recent advances in gel technologies for topical and transdermal drug delivery. Drug Development and Industrial Pharmacy (2014) 40:4, 433–440. [PubMed: 23937582]

46. Swati R, Ankaj K, Vinay P Organogels: Novel Delivery Systems. World Journal of Pharmacy and Pharmaceutical Sciences. (2014) 4, #1:455–471.

47. Davidovich-Pinhas M, Barbut S, Marangoni AG Physical structure and thermal behavior of ethylcellulose. Cellulose (2014) 21, #5:3243–3255.

48. Han L, Li L, Zhao L, et al. Rheological properties of organogels developed by sitosterol and lecithin. Food Research International. (2013) 53, #1:42–28.

49. Moschakis T, Panagiotopoulou E, Katsanidis E, Sunflower oil organogels and organogel-in-water emulsions (part I): Microstructure and mechanical properties. LWT. (2016) 73,:153–161.

50. Rogers M, Wright A, Marangoni A Engineering the oil binding capacity and crystallinity of self-assembled fibrillar networks of 12-hydroxystearic acid in edible oils. Soft Matter. (2008) #4:1483–1490.

51. Almeida I, Bahia M Evaluation of the physical stability of two oleogels. International Journal of Pharmacy. (2006) 327, #1-2:73–77.

52. Davidovich-Pinhas M Oleogels: a promising tool for delivery of hydrophobic bioactive molecules. Therapeutic Delivery. (2016) 7, #1:1–3. [PubMed: 26652617]

53. Marangoni AG, Garti N Edible Oleogels: Structure and Health Implications. AOCS Press; 2018.

54. O'Sullivan CM, Davidovich-Pinhas M Wright A, Barbuta S Marangoni A Ethylcellulose oleogels for lipophilic bioactive delivery – effect of oleogelation on in vitro bioaccessibility and stability of beta-carotene. Food and Function. (2017) 8, #4:1345–1728.

55. Zetzl A, Marangoni A, Barbut S Mechanical properties of ethylcellulose oleogels and their potential for saturated fat reduction in frankfurters. Food & function. (2012) 3, #3:327–37. [PubMed: 22377795]

56. Rogers M, Strober T, Bot A, Toro-Vasquez I, Strotz T, Marangoni A Edible oleogels in molecular gastronomy. International Journal of Gastronomy and Food Science. (2014) 2, #1:22–31.

57. Pehlivano lu H, Demirci M, Toker OS, Konar N, Karasu S, Sagdic O(2018) Oleogels, a promising structured oil for decreasing saturated fatty acid concentrations: Production and food-based applications. Critical Reviews in Food Science and Nutrition. (2018) 58, #8:1330–1341. [PubMed: 27830932]

58. Donati S, Maria Caprani S, Airaghi G, et al. Vitreous Substitutes: The Present and the Future. BioMed Research International. (2014) 2014, Article ID 351804, 12 pages.

59. Wang P, Gao Q, Jiang Z, Lin J, Liu Y, Chen J, Zhou L, Li H, Yang Q and Wang T Biocompatibility and retinal support of a foldable capsular vitreous body injected with saline or silicone oil implanted in rabbit eyes. Clinical & Experimental Ophthalmology. (2012) 40, #1: e67–e75. [PubMed: 21883770]

60. Anand K, Pandey A Validation Study of Steroidal Drugs (Dexamethasone and Betamethasone) by U.V. Spectrophotometric Method. Asian Journal of Pharmaceutical and Clinical Research. (2018) 11, #7:501–505.

61. Friedrich R, Ravanello A, Carlos Cichota L, Rolim C, Beck R Validation of a simple and rapid UV spectrophotometric method for dexamethasone assay in tablets. Química Nova. (2008) 32, #4:1052–1054.

62. Gupta C, Chauhan A Drug transport in HEMA conjunctival inserts containing precipitated drug particles. Journal of Colloid and Interface Science. (2010) 347, #1:31–42. [PubMed: 20381056]

63. Sarao V, Veritti D, Boscia F, Lanzetta P Intravitreal Steroids for the Treatment of Retinal Diseases. The Scientific World Journal. (2014) 2014, Article ID 989501, 14 pages.

64. Rhoades W, Dickson D, Nguyen QD, Do DV Management of macular edema due to central retinal vein occlusion - The role of aflibercept. Taiwan Journal of Ophthalmology. (2017) 7, #2:70–76. [PubMed: 29018760]

65. Zhang Q, Saleh A, Chen J, Sun P, Shen Q Monitoring of thermal behavior and decomposition products of soybean oil: An application of synchronous thermal analyzer coupled with Fourier transform infrared spectrometry and quadrupole mass spectrometry. Journal of Thermal Analysis and Calorimetry. (2014) 115, #1:19–29.

66. Lai HL, Pitt K, Craig D Characterisation of the thermal properties of ethylcellulose using differential scanning and quasi-isothermal calorimetric approaches. International Journal of Pharmaceutics. (2010) 386, #1,2:178–184. [PubMed: 19932159]

67. Chang-Lin J, Attar M, Acheampong A et al. Pharmacokinetics and Pharmacodynamics of a Sustained-Release Dexamethasone Intravitreal Implant. Invest. Ophthalmol. Vis. Sci. (2011) 52, #1:80–86. [PubMed: 20702826]

68. Sarao V, Veritti D, Boscia F, Lanzetta P Intravitreal Steroids for the Treatment of Retinal Diseases. The Scientific World Journal. (2014) 2014, Article ID 989501, 14 pages.

69. Adeniran J, Jusulbegovic D, Schaal S Common and Rare Ocular Side-effects of the Dexamethasone Implant. Ocular Immunology & Inflammation. (2017) 25, #6:834–840. [PubMed: 27379861]

70. Peng CC., Kim J, Chauhan A Extended delivery of hydrophilic drugs from silicone-hydrogel contact lenses containing Vitamin E diffusion barriers. Biomaterials. (2010) 31, #14:4032–4047. [PubMed: 20153894]

71. Ledesema-Duran A, Hernandez S, Santamaria-Holek I Relation between the porosity and tortuosity of a membrane formed by disconnected irregular pores and the spatial diffusion coefficient of the Fick-Jacobs mode. Physical Review. (2017) 95,#5-l: 052804 [PubMed: 28618600]

72. De Backer L, Baron G Effective diffusivity and tortuosity in a porous glass immobilization matrix. Applied Microbiology and Biotechnology. (1993) 39,:281–284.

73. Shen L, Chen Z Critical review of the impact of tortuosity on diffusion. Chemical Engineering Science. (2007) 62, #14:3748–3755.

74. Lim P, Barbour S, Fredlund D The influence of degree of saturation on the coefficient of aqueous diffusion. Canadian Geotechnical Journa., (1998) 35, #5:811–827.

75. Yorston D Anti-VEGF drugs in the prevention of blindness. Community Eye Health. (2014) 27, #87:44–46. [PubMed: 25918459]

76. Lanzetta P, Loewenstein A; Vision Academy Steering Committee. Fundamental principles of an anti-VEGF treatment regimen: optimal application of intravitreal anti-vascular endothelial growth factor therapy of macular diseases. Graefes Arch Clin Exp Ophthalmol. (2017) 255, #7:1259–1273. [PubMed: 28527040]

77. Lee SS, Hughes P, Ross AD et al. Biodegradable Implants for Sustained Drug Release in the Eye. Pharm Res. (2010) 27, #10: 2043–2053. [PubMed: 20535532]

78. Karabas V, özkan B, Koçer C, Altmta O, Pirhan D, Yüksel N Comparison of Two Anesthetic Methods for Intravitreal Ozurdex Injection. Journal of Ophthalmology. (2015) 2015, Article ID 861535, 5 pages.

79. Moisseiev E, Regenbogen M, Rabinovitch T, Barak A, Loewenstein A, Goldstein M Evaluation of pain during intravitreal Ozurdex injections vs. intravitreal bevacizumab injections. Eye (Lond). (2014) 28, #8:980–985. [PubMed: 24924442]

80. Zheng A, Chin EK, Almeida DR, Tsang SH, Mahajan VB Combined Vitrectomy and Intravitreal Dexamethasone (Ozurdex) Sustained-Release Implant. Retina. (2016) 36, #11:2087–2092. [PubMed: 27148836]
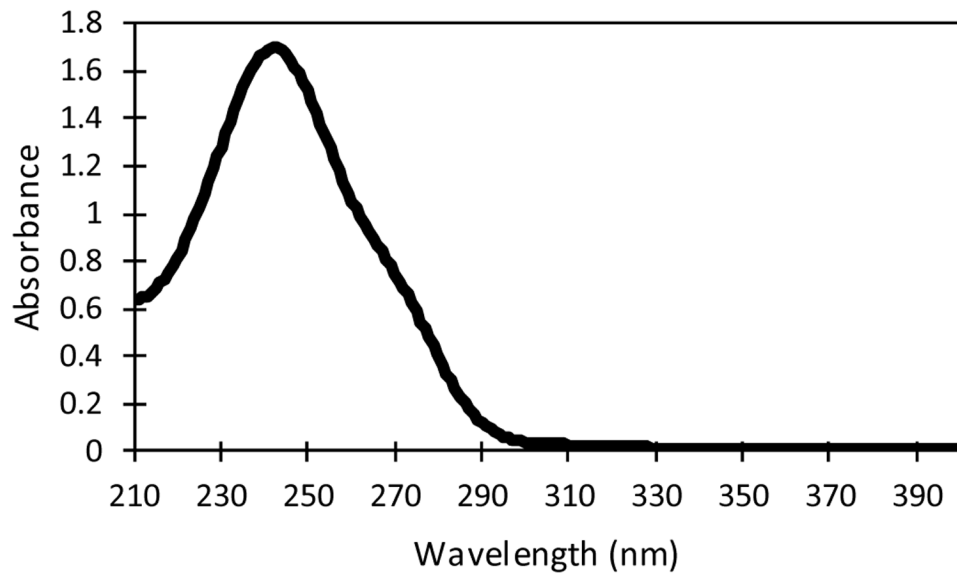
Figure 1:
Absorbance spectra of dexamethasone at 0.05 mg/mL in PBS 1X.
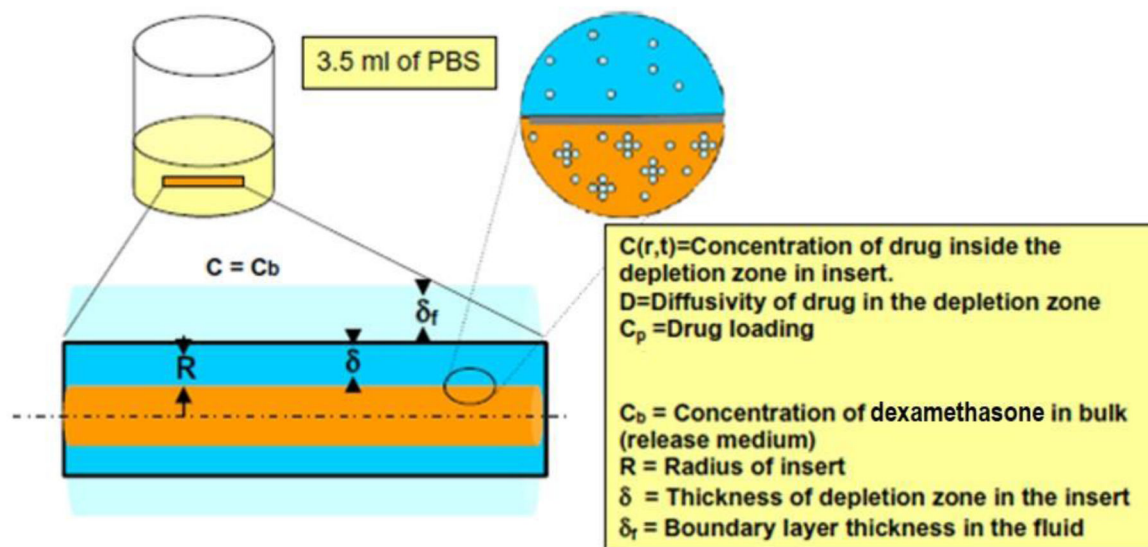
Figure 2:
Model geometry illustrating drug diffusion from the particle loaded cylindrical oleogel device to the surrounding fluid. Diffusion of dissolved drug into the fluid results in dissolution of particles creating a shell of depletion zone with a core of particle-containing gel.
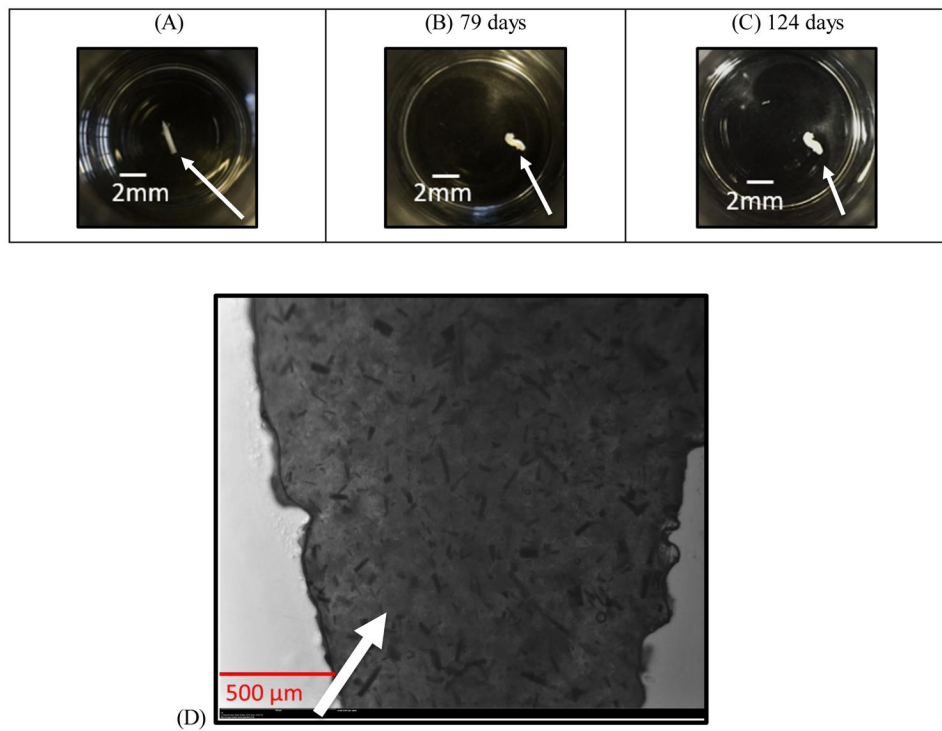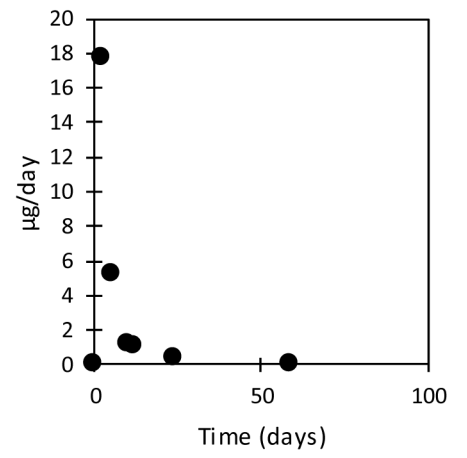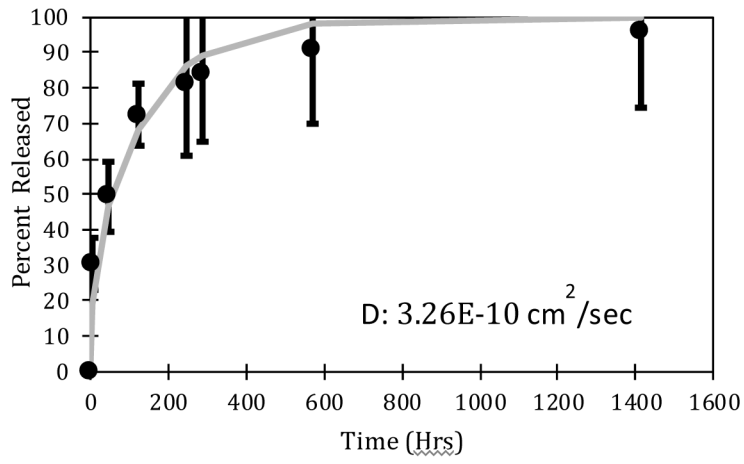
Figure 3(A, B, C, D):
Snapshots of the dexamethasone loaded (28% w/w) device expunged through a 22 gauge needle at various times. (A) t = 0, (B) 79 days, (C) 124 days. (D) Microscopic image of the dexamethasone drug gel formulation at 28% loading under 2x magnification.

Figure 4:
Photograph of the dexamethasone device on human thumb. Size of the device is set by needle gauge size and desired mass of oleogel. The devices appear white due to the presence of the dexamethasone particles.
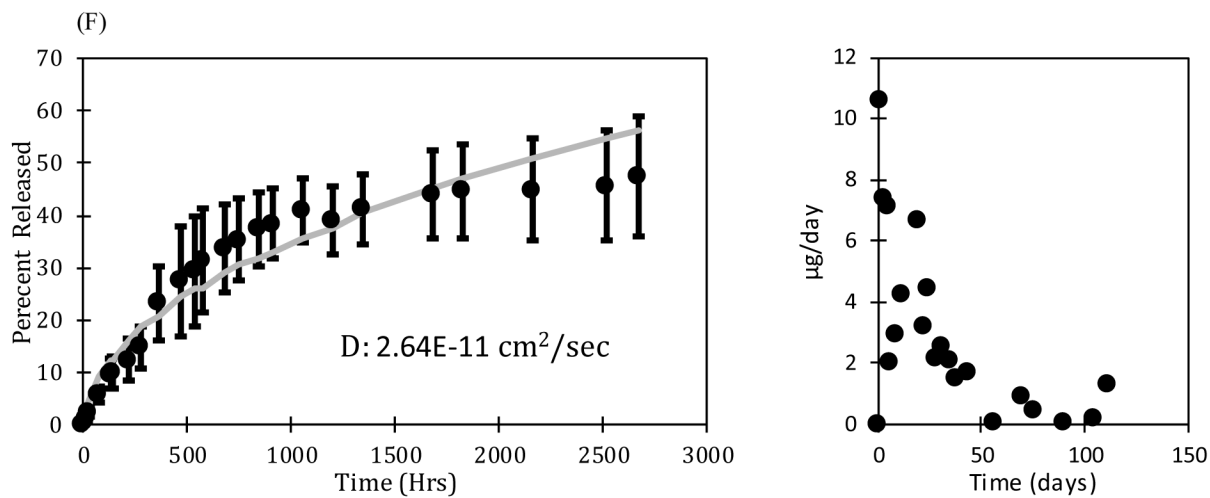
(A)

D: $3.26E\text{-}10 \text{ cm}^2/\text{sec}$

(B)

D: $5.81E\text{-}11 \text{ cm}^2/\text{sec}$

(C)

D: 5.28E-11 cm^2/sec

(D)

D: 4.29E-11 cm^2/sec

(E)

D: 4.24E-11 cm^2/sec

(F)

$$D: 2.64E\text{-}11 \ cm^2/sec$$
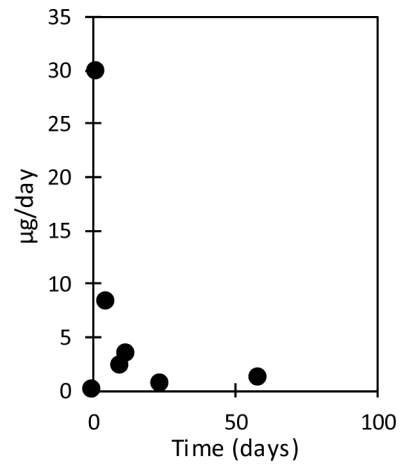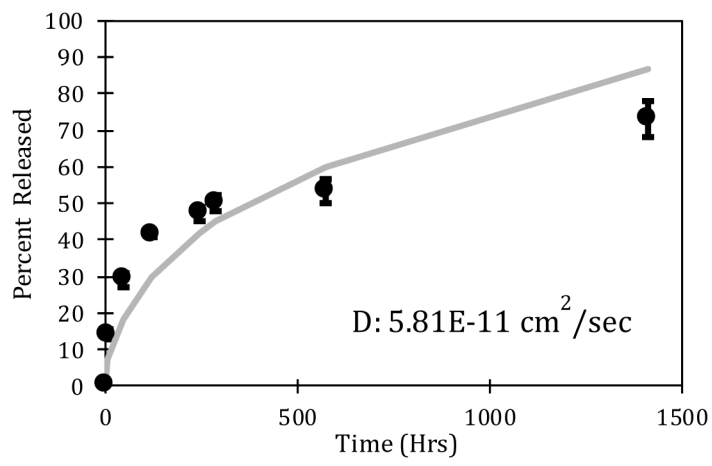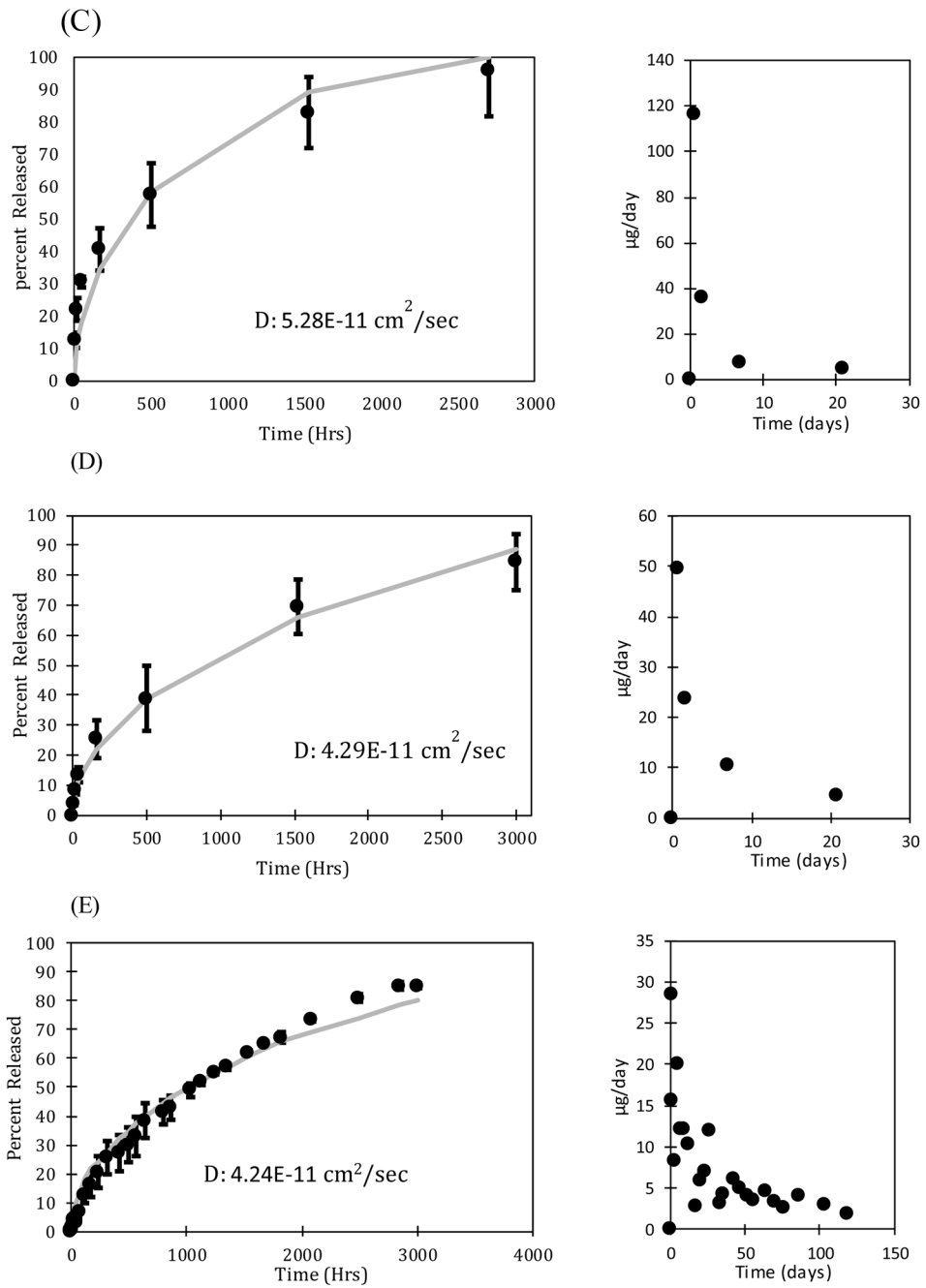
FIGURE 5 (A, B, C, D, E, F):

Release profiles and release rates per day for (A) 3% (= 70 μg) (B) 5% (= 160 μg) (C) 10% (= 400 μg), (D) 15% (= 450 μg), (E) 28% (= 700 μg), and (F) 40% (= 360 μg) dexamethasone loading. The mass of drug loaded can be controlled without impacting the release duration by changing the length of the device. The error bars are calculated from the standard deviation of three independent experiments.
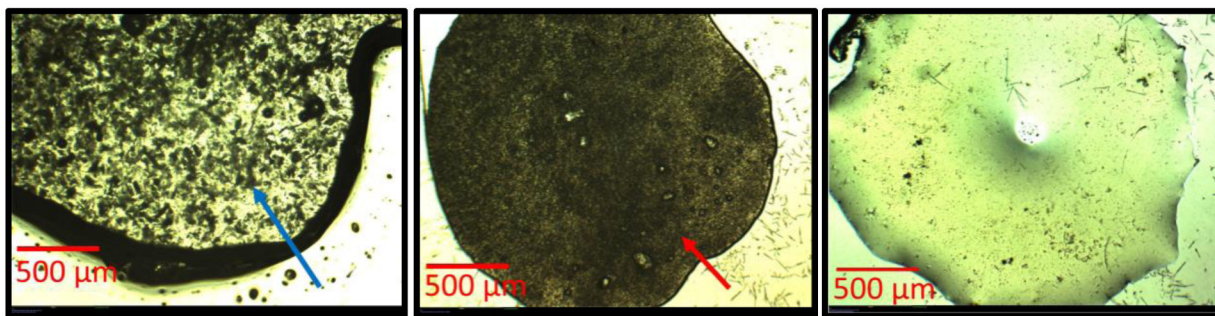
Figure 6 (A, B, C):

All images are shown at 2x magnification. (A) Freshly formulated 5% drug loading dexamethasone oleogel showing presence of particles (blue arrow) (B) Gel in (A) after 4 months drug release. Particles are no longer visible, but have been replaced by small circular voids that are smaller in size and more uniformity in shape. The red arrow points to one of the many voids located throughout the gel. (C) Gel in (B) after melting and solidification. Voids are no longer visible because the oil phase filled the spaces during the melting process.
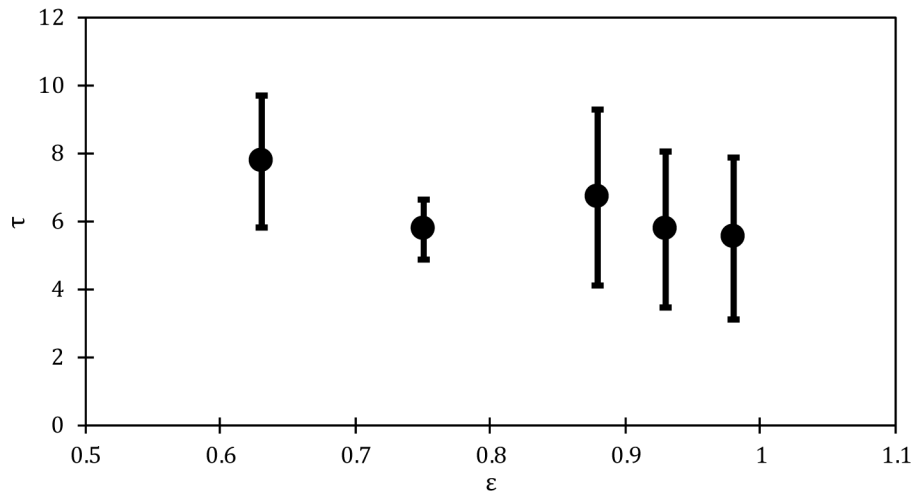
Figure 7:
Dependency of the tortuosity on porosity in the particle loaded oleogels. Error bars are calculated from the standard deviation of three independent experiments.
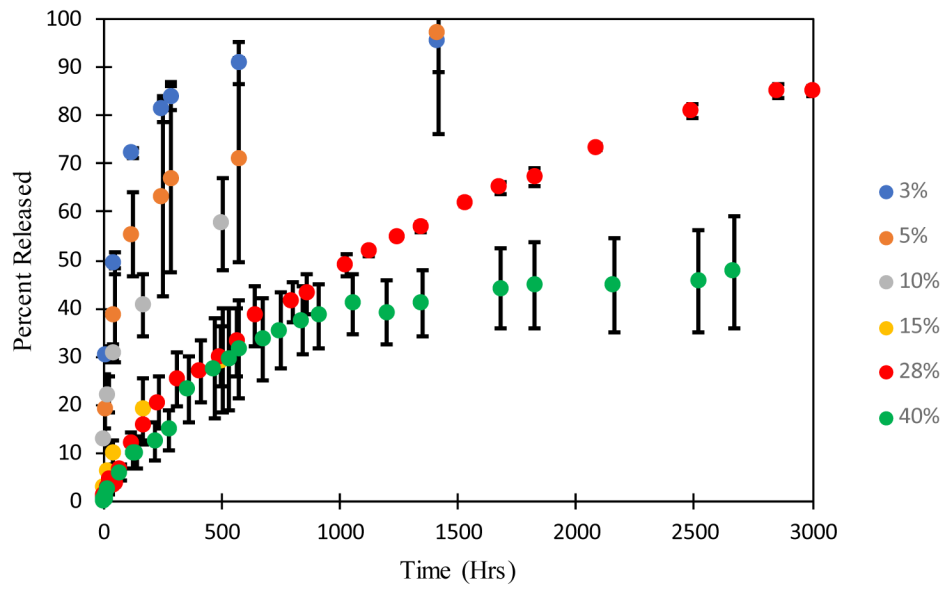
Figure 8:
Effect of drug loading on dexamethasone release profiles. Error for each drug loading is estimated from the standard deviation of three independent experiments.

Table 1:

Solubility of Drug tested in Water and in the Oil Phase of the Oleogel

Name of Drug	Indications	Solubility Limit in PBS @ 25°C	Solubility Limit in Oil Phase of Oleogel
Dexamethasone	Central Retinal Vein Occlusion, Macular Edema, Diabetic Macular Edema, Uveitis [63,64]	89 μg/mL	30 mg/mL